Kinetic Mechanism of Enterococcal Aminoglycoside Phosphotransferase 2″-Ib†

Marta Toth,‡ Jaroslav Zajicek,‡ Choonkeun Kim,‡ Joseph W. Chow,§ Clyde Smith,|| Shahriar Mobashery,‡ and Sergei Vakulenko*,‡

Department of Chemistry and Biochemistry, University of Notre Dame, Notre Dame, Indiana 46556, Department of Infectious Diseases Clinical Research, Merck Research Laboratories, North Wales, Pennsylvania 19454-109, and Stanford Synchrotron Radiation Laboratory, Menlo Park, California 94025

Received November 28, 2006; Revised Manuscript Received February 15, 2007

ABSTRACT: The major mechanism of resistance to aminoglycosides in clinical bacterial isolates is the covalent modification of these antibiotics by enzymes produced by the bacteria. Aminoglycoside 2″-Ib phosphotransferase [APH(2″)-Ib] produces resistance to several clinically important aminoglycosides in both Gram-positive and Gram-negative bacteria. Nuclear magnetic resonance analysis of the product of kanamycin A phosphorylation revealed that modification occurs at the 2″-hydroxyl of the aminoglycoside. APH(2″)-Ib phosphorylates 4,6-disubstituted aminoglycosides with k_{cat}/K_m values of 10^5-10^7 M^{-1} s^{-1}, while 4,5-disubstituted antibiotics are not substrates for the enzyme. Initial velocity studies demonstrate that APH(2″)-Ib operates by a sequential mechanism. Product and dead-end inhibition patterns indicate that binding of aminoglycoside antibiotic and ATP occurs in a random manner. These data, together with the results of solvent isotope and viscosity effect studies, demonstrate that APH(2″)-Ib follows the random Bi−Bi kinetic mechanism and substrate binding and/or product release could limit the rate of reaction.

Antibiotic-resistant enterococci are among the most common bacteria isolated in nosocomial infections in the United States, and have emerged as a major therapeutic challenge (*1*, *2*). Optimal antimicrobial therapy for serious enterococcal infections requires the use of synergistic combinations of a cell wall active agent, such as ampicillin or vancomycin, with an aminoglycoside, which results in bactericidal activity against the enterococci. However, many enterococcal strains have acquired aminoglycoside resistance genes that encode aminoglycoside-modifying enzymes, which eliminate this synergistic bactericidal effect. Thus, in many medical centers high-level resistance to aminoglycosides has precluded optimal therapy for the majority of enterococcal infections.

High-level resistance to the aminoglycoside gentamicin in enterococci is mediated by APH(2″)[1] enzymes. The first aminoglycoside 2″-phosphotransferase discovered in enterococci was mediated by a single gene, *aac(6′)-Ie-aph*(2″)*-Ia*, which encodes the bifunctional enzyme, AAC(6′)-Ie-APH-(2″)-Ia. This enzyme possesses both 6′-acetylating and 2″-phosphorylating activities (*3*, *4*). Enterococcal strains harboring this gene exhibit high-level resistance to virtually all clinically available aminoglycosides, including gentamicin, amikacin, kanamycin A, tobramycin, netilmicin, and dibekacin, but not to streptomycin (*5*, *6*). The two enzymatic domains of the *aac(6′)-Ie-aph*(2″)*-Ia* gene have been separately cloned and expressed. The APH(2″)-Ia enzyme demonstrates extremely broad substrate range as well as the regiospecificity for phosphate transfer (*7*, *8*). Phosphorylation by this enzyme occurs at the 2″-OH of 4,6-disubstituted aminoglycosides (kanamycin A). The 4,5-disubstituted aminoglycoside neomycin was phosphorylated at 3′-OH (primarily) and 3‴-OH and another 4,5-disubstituted aminoglycoside (lividomycin) at position 5″−OH. The phosphotransferase reaction of the bifunctional enzyme AAC(6′)-Ie-APH-(2″)-Ia was proposed to operate by a random rapid equilibrium mechanism, where either one of the two substrates (aminoglycoside antibiotic or ATP) can bind to the enzyme first.

More recently three other *aph(2″)* aminoglycoside resistance genes, *aph(2″)-Ib*, *-Ic*, and *-Id*, were discovered in enterococci (*9*−*11*). Regiospecificity of phosphate transfer by these enzymes had been predicted to be at the 2″-OH position, based on the relatively low (24−33%) amino acid identity with the APH(2″)-Ia domain of the bifunctional enzyme AAC(6′)-Ie-APH(2″)-Ia. In this study we describe cloning and purification of APH(2″)-Ib, characterization of its substrate specificity, and the nature of the regiospecificity of phosphoryl transfer. We also employed initial velocity patterns, inhibition studies, and solvent isotope, thio, and solvent viscosity effects to evaluate the kinetic mechanism of this aminoglycoside phosphotransferase.

† This research was funded by a grant from the National Institutes of Health.

* Corresponding author. Tel: (574) 631-2935. Fax: (574) 631-6652 E-mail: svakulen@nd.edu.

‡ University of Notre Dame.

§ Merck Research Laboratories.

|| Stanford Synchrotron Radiation Laboratory.

[1] Abbreviations: APH, aminoglycoside phosphotransferase; LB, Luria−Bertani medium; APH, aminoglycoside phosphotransferase; IPTG, isopropyl-β-D-thiogalactopyranoside; ATP, adenosine 5′-triphosphate; ADP, adenosine 5′-diphosphate; AMP-PCP, β,γ-methyleneadenosine 5′-triphosphate; ATPγS, adenosine 5′-(3-thiotriphosphate); HEPES, *N*-(2-hydroxyethyl)piperazine-*N*′-2-ethanesulfonic acid; PEP, phosphoenolpyruvate; LD, lactate dehydrogenase; PK, pyruvate kinase; NADH, β-nicotinamide-adenine dinucleotide (reduced); NMR, nuclear magnetic resonance; PEG 8000, polyethyleneglycol average molecular weight 8000; TLC, thin-layer chromatography.

10.1021/bi6024512 CCC: $37.00
Published on Web 04/11/2007

EXPERIMENTAL PROCEDURES

Cloning of the aph(2″)-Ib Gene into Expression Vector. The *aph(2″)-Ib* gene, previously cloned into the pBluescript II KS(+) vector, was utilized as a template for cloning into the expression vector (*10*). First, we abolished the single *Nde*I site within the *aph(2″)-Ib* by site-directed mutagenesis without changing the amino acid sequence of the encoded APH(2″)-Ib enzyme. The resulting gene was PCR-amplified by high-fidelity Pfu Turbo polymerase (Stratagene), using two synthesized oligonucleotide primers: 2″IbNde (TATCATATGGTTAACTTGGACGCTGAG; *Nde*I site underlined) and 2″IbEcoR1 (TATGAATTCCTGCTAAAATATAAACATC; *Eco*RI site underlined). The amplified DNA fragment was digested with *Nde*I and *Eco*RI and cloned into the unique *Nde*I−*Eco*RI sites of the pET22b(+) vector (Novagen) to produce pET:APH(2″)-Ib. After transformation into the recipient strain *Escherichia coli* JM83 and selection on LB agar supplemented with 100 μg/mL of ampicillin, the nucleotide sequence of the cloned *aph(2″)-Ib* gene was verified by sequencing of both DNA strands. To achieve a higher level of protein expression, the pET:APH(2″)-Ib construct was retransformed into *E. coli* BL21(DE3) and selection was performed on LB agar supplemented with 100 μg/mL of ampicillin.

Purification of APH(2″)-Ib Phosphotransferase. First, a small-scale pilot experiment was performed to determine the optimal temperature for protein expression. Bacteria were grown overnight in 5 mL of LB broth supplemented with IPTG (0.4 mM) and ampicillin (200 μg/mL) at three different temperatures (5 °C, 25 °C, and 37 °C). One milliliter of bacterial culture was sonicated for 1 min (Bronson Sonifier 450; VWR, West Chester, PA) to disrupt cells and centrifuged at 20000*g* for 5 min. A 25 μL portion of the supernatant was subjected to a mini SDS−PAGE, and relative levels of protein expression were evaluated. Based on this experiment, for large-scale protein purification, induction with IPTG was performed at 25 °C overnight. Bacteria were pelleted by centrifugation, and cells were disrupted by sonication. After centrifugation at 20000*g* for 30 min, the APH(2″)-Ib enzyme was purified from the supernatant by affinity chromatography with gentamicin as the bound ligand, according to a recent procedure (*12*). Fractions were examined by SDS−PAGE, and those that contained the APH(2″)-Ib protein were pooled, concentrated to the final volume of 20 mL, and dialyzed twice against 5 L of 25 mM sodium HEPES, pH 7.5.

Preparation and Purification of Phosphorylated Kanamycin. Kanamycin phosphate was prepared by incubating 40 mg of kanamycin A in 10 mL of reaction mixture containing 100 mM sodium HEPES, pH 7.5, 20 mM KCl, 10 mM ATP, 20 mM $MgCl_2$, 40 mM phosphoenolpyruvate (PEP), 80 units of pyruvate kinase (PK), and 15 μL of 32 μM solution of purified enzyme. The reaction proceeded at room temperature, and the extent of kanamycin A phosphorylation was monitored by thin-layer chromatography (TLC) using a mixture of ethanol, methanol, ammonium hydroxide, and water at a 1:1:0.9:0.9 ratio and with nonmodified kanamycin A as a control. The TLC plate was dried on a thermo plate and developed with ninhydrin. The reaction mixture was supplemented twice (after 2 and 4 h of incubation) with additional amounts of enzyme (15 μL of a 32 μM solution) and PK (80 units) and left overnight at room temperature. Upon complete phosphorylation of kanamycin A the reaction mixture was filtered first through 30 kDa and then through 10 kDa filters to remove the enzymes. This mixture was then applied to a silica gel layer (20 g of silica gel in 60 mL fritted glass filter) and drained under low vacuum (water aspirator). The silica gel was washed with 200 mL of a methanol−water (1:1) mixture under vacuum, and kanamycin phosphate was eluted with 50 mL of methanol−water−ammonium hydroxide mixture (1:1:1) under vacuum. The collected fraction was dried in a rotary evaporator at room temperature and dissolved in 8 mL of water. This solution then was centrifuged at 20000*g* for 20 min to remove insoluble impurities and was applied to an Amberlite CG 50 ion exchange column (3 × 12 cm; Bio-Rad). The column was prepared by activating the Amberlite CG 50 with 1% of NH_4OH (by stirring the resin 3 times in 100 mL of 1% of NH_4OH for 10 min each), followed by washing with 400 mL of water. After application of the sample, the column was washed with 300 mL of water and kanamycin phosphate was eluted using a stepwise gradient (0.4, 0.6, 0.8, 1.0, 1.2, 1.4, 1.6, 1.8, 2.0, and 3%; 30 mL for each concentration) of NH_4OH. All fractions were analyzed by TLC, and those containing kanamycin phosphate were combined and dried *in vacuo*. The pellet was dissolved in 1 mL of water and was applied to a G10 Sephadex (Sigma) column (1 × 120 cm; Bio-Rad) and washed with water. Fractions (0.5 mL each) were analyzed by TLC, and those containing the modified kanamycin A were pooled and dried.

NMR Spectroscopy. Kanamycin phosphate, 6.5 mg, was dissolved in 10 mL of D_2O (^2H 99.9%), supplemented with 0.001% of dimethylsilapentane-5 sulfonic acid sodium salt (DSS) and lyophilized. The residue was dissolved in D_2O and was lyophilized again. Finally, the pellet was dissolved in 700 μL of deuterium oxide for the analysis (^2H 99.96%).

All ^1H and ^{13}C NMR experiments were performed at 25 °C using Varian UnityPlus and Bruker AVANCE spectrometers operating at ^1H resonance frequency of 599.89 and 800.13 MHz, respectively. Various 1D and 2D homo- and heteronuclear NMR techniques, ^1H, $^1H\{^{31}P\}$, $^{13}C\{^1H\}$, $^1H-^1H$ DQF-COSY, $^1H-^1H$ TOCSY, $^1H-^{13}C$ gHMQC, and $^1H-^{13}C$ gHMBC, were employed to elucidate the structure of the modified kanamycin A in deuterium oxide. Standard pulse sequences were used in these experiments (*13*−*18*). Time domain data (t_2 and t_1) for all 2D experiments were recorded as $2k \times 1k$ complex matrices with 4 or 8 scans per t_1 increment. The relaxation delay between individual scans was 1.2 s. In homonuclear 2D experiments, zero filling was used in both t_2 and t_1 domains to obtain final $4k \times 2k$ complex time domain data. In heteronuclear 2D experiments, linear prediction to the 2048 complex data points was applied in the t_1 domain, which was zero filled to 4096 to obtain the final $2k \times 4k$ complex time domain data. Shifted sine bell weighting functions were applied in both domains prior to double Fourier transformation. Spectra measured with the Varian and Bruker spectrometers were processed using Varian VNMR 6.1C and Bruker TopSpin 1.3 softwares, respectively. ^1H spectra and the ^1H dimension in 2D heteronuclear spectra were referenced relative to the signal of DSS (internal standard, $\delta = 0$ ppm). ^{13}C spectra and the ^{13}C dimension in the 2D heteronuclear spectra were referenced indirectly (*19*).

2″-O-(Phosphoryl)kanamycin. ^{1}H NMR (800 MHz, D_2O): δ ppm 5.48 (1H, d, $^3J_{H-1',H-2'} = 3.9$ Hz, H-1′), 5.24 (1H, d, $^3J_{H-1'',H-2''} = 3.7$ Hz, H-1″), 4.01 (1H, td, $^3J_{H-2'',H-3''} = 10.2$ Hz, $^3J_{H-2'',P} = 9.8$ Hz, H-2″), 3.97 (1H, mt, $^3J_{H-5'',Ha-6''} = 2.3$ Hz, $^3J_{H-5'',Hb-6''} = 4.7$ Hz, H-5″), 3.91 (1H, mt, $^3J_{H-5',Ha-6'} = 8.9$ Hz, $^3J_{H-5',Hb-6'} = 2.8$ Hz, H-5′), 3.81 (1H, dd, $^{gem}J_{Ha-6'',Hb-6''} = 12.4$ Hz, H_a-6″), 3.77 (1H, dd, H_b-6″), 3.76 (1H, t, $^3J_{H-5,H-6} = 9.2$ Hz, H-5), 3.73 (1H, t, $^3J_{H-3',H-4'} = 9.6$ Hz, H-3′), 3.61 (1H, dd, $^3J_{H-2',H-3'} = 9.8$ Hz, H-2′), 3.58 (1H, t, H-6), 3.57 (1H, t, $^3J_{H-4'',H-5''} = 10.1$ Hz, H-4″), 3.45 (1H, t, $^3J_{H-4,H-5} = 9.5$ Hz, H-4), 3.33 (1H, t, $^3J_{H-4',H-5'} = 9.6$ Hz, H-4′), 3.28 (1H, t, $^3J_{H-3'',H-4''} = 10.5$ Hz, H-3″), 3.25 (1H, mt, $^3J_{H-3,H-4} = 9.6$ Hz, H-3), 3.24 (1H, dd, $^{gem}J_{Ha-6',Hb-6'} = 13.5$ Hz, H_a-6′), 3.00 (1H, mt, $^3J_{H-1,Ha-2} = 4.8$ Hz, $^3J_{H-1,Hb-2} = 12.4$ Hz, $^3J_{H-1,H-6} = 9.7$ Hz, H-1), 2.99 (1H, dd, H_b-6′), 2.13 (1H, dt, $^{gem}J_{Ha-2,Hb-2} = 12.6$ Hz, $^3J_{Ha-2,H-3} = 5.0$ Hz, H_a-2), 1.44 (1H, q, $^3J_{Hb-2,H-3} = 12.4$ Hz, H_b-2).

^{13}C NMR (201 MHz, D_2O): δ ppm 98.23 (d, $^3J_{C-1'',P} = 2.3$ Hz, C-1″), 97.71 (C-1′), 84.72 (C-6), 83.81 (C-4), 73.65 (C-5), 72.04 (d, $^2J_{C-2'',P} = 5.6$ Hz, C-2″), 71.97 (C-3′), 71.82 (C-5″), 70.99 (C-2′), 70.55 (C-4′), 69.90 (C-5′), 67.29 (C-4″), 59.58 (C-6″), 53.73 (d, $^3J_{C-3'',P} = 4.7$ Hz, C-3″), 49.54 (C-3), 47.98 (C-1), 40.39 (C-6′), 32.67 (C-2).

Enzyme Assay and Initial Velocity Patterns. We employed the continuous spectrophotometric assay to monitor phosphorylation of aminoglycoside antibiotics by APH(2″)-Ib. In the continuous assay, the production of ADP during phosphorylation of aminoglycoside is measured as a function of NADH oxidation (decrease in the absorbance of NADH at 340 nm) by coupling pyruvate kinase with lactic dehydrogenase (LD). This assay involves regeneration of ATP, and thus avoids the possibility of inhibition by ADP or a diminution of the ATP concentration in the course of turnover. All kinetics assays were performed in a total volume of 250 μL containing 100 mM sodium HEPES, pH 7.5, 10 mM $MgCl_2$, 20 mM KCl, 2 mM PEP, 100 μM NADH, 10 units/mL PK, 24 units/mL LD, 100 μM ATP, and varying the concentrations of the aminoglycoside substrates. The reaction was initiated by adding enzyme (final concentration of 4 nM). Kinetic parameters for ATP were determined using the same reaction conditions, except by fixing the kanamycin A concentration at 10 μM and varying the concentrations of ATP. The K_m and k_{cat} values were obtained by nonlinear regression using the Grafit 4.0 software.

Initial velocity patterns for APH(2″)-Ib were obtained by measuring the rates of reaction at three different fixed concentrations of ATP (8, 16, and 32 μM) and variable concentrations of amikacin (from 20 to160 μM). Enzyme was used at a final concentration of 10 nM.

Inhibition Studies. To investigate the order of substrate binding, inhibition studies with dead-end inhibitors neamine and AMP-PCP were conducted. Measurements were performed at several fixed concentrations of inhibitor. When neamine or AMP-PCP was tested as the inhibitor against isepamicin, the concentration of isepamicin was varied between 10 and 80 μM, while ATP was used at a constant concentration of 16 or 20 μM. When neamine or AMP-PCP was tested as the inhibitor versus ATP, the concentration of ATP was varied between 10 and 80 μM and the concentration of isepamicin was kept at 15 μM. To investigate the order of product release, kanamycin phosphate was used as the inhibitor against ATP and isepamicin. As with the dead-end inhibitors, kanamycin phosphate was used at several fixed concentrations, while concentration of one of the substrates was varied, and the other substrate was used at a constant concentration around its K_m value (16 μM for ATP and 15 μM for isepamicin).

Solvent Isotope Effects. To elucidate the solvent isotope effects, we carried out reactions in water and in deuterium oxide at fixed saturating concentration of ATP (100 μM) or kanamycin A (40 μM) and variable concentrations of kanamycin A (2.5, 3.5, 5, 10, and 20 μM) or ATPγS (20, 40, 60, and 80 μM). When kanamycin A was used as variable substrate, experiments in water were performed at pH values 6.5 and 7.5. When we used deuterium oxide, we adjusted pH to 6.1 and 7.1 so corresponding pD values (pH meter reading plus 0.4) were also 6.5 and 7.5. When ATPγS was used as variable substrate, experiments were performed at pH and pD value of 7.0.

Viscosity Effects. The effect of solvent viscosity was determined in the presence of glycerol and PEG 8000. Glycerol was used at four concentrations, 8, 16, 24, and 32%, that corresponds to relative viscosities (η) of 1.2, 1.5, 2.0, and 2.6 (*20*). PEG 8000 was used at a concentration of 6.7% ($\eta = 3.6$). Assays were performed at a fixed concentration of either kanamycin A (20 μM) or ATP (100 μM) and variable concentrations of ATP (10−80 μM), kanamycin A (2−20 μM), amikacin (20−160 μM), or ATPγS (20−80 μM).

Thio Effects. For elucidation of thio effects we uncoupled the assay by omitting PEP from the reaction mixture. We used kanamycin A at a fixed concentration (100 μM) and adenosine 5′-(3-thiotriphosphate) (ATPγS) instead of ATP at four concentrations (25, 50, 100, and 200 μM). APH(2″)-Ib was used at 200 nM.

Data Analysis. Data for steady-state kinetics were fit to eq 1 using Grafit 4.0 software (Erithacus Software, Staines, U.K.). Initial velocity data were fit to eq 2 while data for competitive, uncompetitive, and noncompetitive inhibition were fit to eqs 3−5, respectively (*21*). v is the initial velocity,

$$v = V_m[A]/(K_a + [A]) \quad (1)$$

$$v = V_m[A][B]/(K_a[B] + K_b[A] + [A][B] + K_{ia}K_b) \quad (2)$$

$$v = V_m[A]/([A] + K_a(1 + [I]/K_{is})) \quad (3)$$

$$v = V_m[A]/(K_a + [A]/(1 + [I]/K_{ii})) \quad (4)$$

$$v = V_m[A]/(K_a(1 + [I]/K_{is}) + [A](1 + [I]/K_{ii})) \quad (5)$$

V_m is the maximum velocity, [I] is the concentration of inhibitor, [A] and [B] are the concentrations of substrates, K_a and K_b are the corresponding Michaelis−Menten constants, and K_{ia} is the dissociation constant for A. K_{is} and K_{ii} are the slope and intercept inhibition constants obtained by replotting the values for the slope and intercept from double-reciprocal plots versus inhibitor concentration.

RESULTS AND DISCUSSION

Enzyme Isolation and Storage. Using a one-step affinity purification procedure we obtained 20 mg of homogeneously

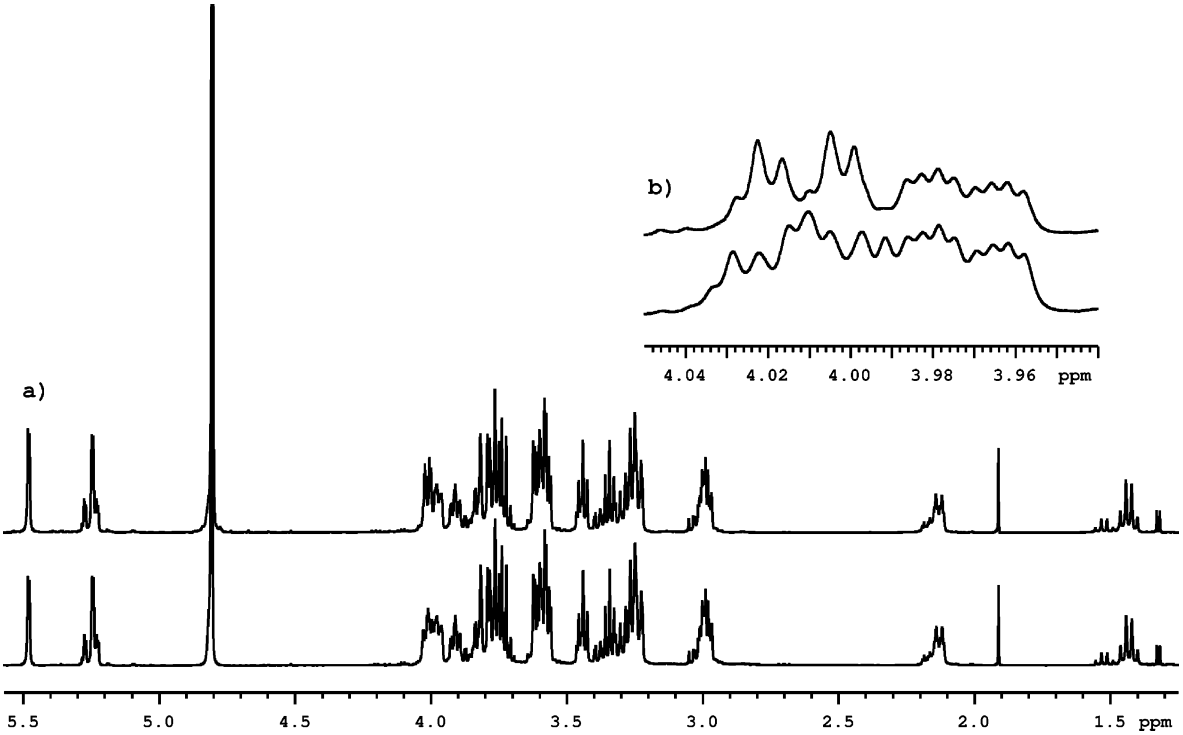

FIGURE 1: (a) Full ^{1}H (bottom) and ^{1}H{^{31}P} (top) NMR spectra of phosphorylated kanamycin A. (b) The inset is an expanded region showing the H-2″ proton signal at δ 4.01 ppm; ^{1}H spectrum (bottom), ^{1}H{^{31}P} spectrum (top).

pure APH(2″)-Ib enzyme from 400 mL of an overnight bacterial culture. The enzyme was stored in liquid nitrogen at a concentration of 32 μM in 33% of glycerol. Under these conditions it was stable for at least 1 year. When stock enzyme solution was diluted for kinetic assays, it was stabilized by supplementing the solution with 0.2 mg/mL of acetylated BSA.

NMR Analysis. Kanamycin A was phosphorylated in the presence of the enzyme and ATP. The product of the reaction was purified, and its structure was determined by analysis of 1D and 2D ^{1}H and ^{13}C NMR spectra. Proton connectivities were derived by examination of the DQF-COSY and TOCSY spectra. Signals of all carbons with directly attached protons were assigned using the gHMQC spectrum. Finally, the gHMBC spectrum was used to assign quaternary carbons and to check the correctness of the connectivities established by the interpretation of the other spectra.

The ^{1}H spectrum of this compound (Figure 1) showed two one proton doublets at δ 5.24 and 5.48, which were assigned to the anomeric protons of 3-amino-3-deoxyglucose and 6-amino-6-deoxyglucose, respectively. Signals of the remaining protons of these moieties were assigned by analyzing the DQF-COSY and TOCSY spectra. The C2 methylene proton signals of the 2-deoxystreptamine moiety were identified in the COSY spectrum at δ 1.44 and 2.13. They showed a mutual cross-peak, and both exhibited cross-peaks to the C1 and C3 methine proton signals at δ 3.00 and 3.25, respectively. Following the interpretation of the TOCSY spectrum, the C4, C5, and C6 methine proton signals of this moiety were assigned. By analyzing the gHMQC spectrum, the signals of all carbons with directly attached protons were unambiguously assigned. In the gHMBC spectrum, the resonance of the anomeric proton of the 6-amino-6-deoxyglucose moiety showed a cross-peak with the carbon signal at δ 84.2 corresponding to the C4 carbon of the 2-deoxystreptamine moiety. Simultaneously, the signal (δ 85.1) of the C6 carbon of this moiety exhibited a cross-peak with the anomeric proton signal of the 3-amino-3-deoxyglucose (δ 5.24).

Comparison of the 1D ^{1}H and ^{1}H{^{31}P} spectra revealed that a triplet of doublet ($^3J_{H-1'',H-2''} = 3.7$ Hz, $^3J_{H-2'',H-3''} = 10.2$ Hz, $^3J_{H-2'',P} = 9.8$ Hz) corresponding to the H2″ proton collapses into a doublet of doublet ($^3J_{H-1'',H-2''} = 3.7$ Hz, $^3J_{H-2'',H-3''} = 10.2$ Hz) when the proton spectrum is measured with broadband phosphorus decoupling (Figure 1). Moreover, the C1″, C2″, and C3″ carbon signals showed as doublets in the ^{13}C{^{1}H} spectrum with $^3J_{C-1'',P} = 2.3$ Hz, $^2J_{C-2'',P} = 5.6$ Hz, and $^3J_{C-3'',P} = 4.7$ Hz, respectively, due to spin−spin interaction between ^{31}P and the corresponding ^{13}C nuclei. These facts unambiguously revealed that the phospho group is attached to the C2″ carbon of the 3-amino-3-deoxyglucose moiety (Figure 2).

It is important to state that, despite the fact that the product of kanamycin A phosphorylation was pure, we noted some satellite peaks in the spectrum. For example, the quartet at δ 1.44 has a minor partner in the quartet at δ 1.52. There are other examples such as this for the remaining resonances. A change in temperature (up to 65 °C) did not merge the two sets of signals, indicating that these were not merely due to conformational states of the rings in the structure. However, an increase of the pD of the solution to the value of 12.4 merged the two sets of resonances. We conclude that phosphorylated kanamycin in the deuterium oxide solution at pD values lower than the above value exists in a major and a minor form. The minor form is likely a form where the phosphate ester exists as an ion pair with one of the amines of the antibiotic itself, fixing the amine in this complex as an ammonium species. The increase in pH abrogates this interaction, hence simplifying the spectrum.

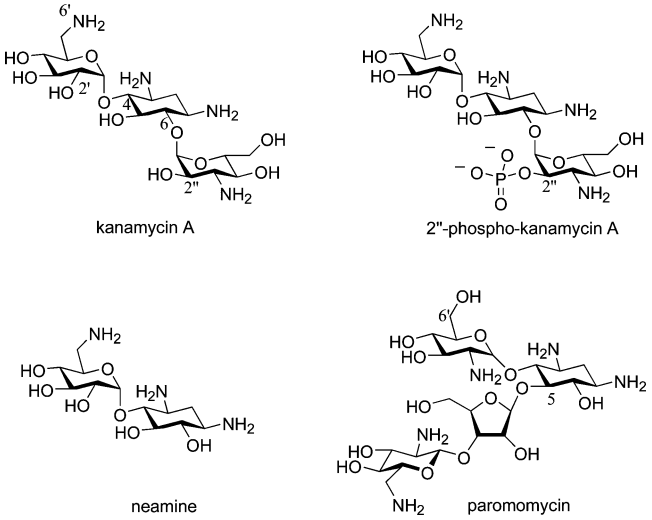

FIGURE 2: Structures of three aminoglycoside antibiotics and 2″-phosphoryl kanamycin A.

The observed vicinal couplings $^3J_{H-2'',P} = 9.8$ Hz, $^3J_{C-1'',P} = 2.3$ Hz, and $^3J_{C-3'',P} = 4.7$ Hz can be interpreted in terms of preferred orientation of the phosphoryl group in the above moiety. Karplus equations for the corresponding P−O−C−H and P−O−C−C fragments

$$^3J_{POCH} = 15.3 \cos^2 \theta - 6.1 \cos \theta + 1.6$$

$$^3J_{POCC} = 6.9 \cos^2 \theta - 3.4 \cos \theta + 0.7$$

indicate that the dihedral angle between the P−O and C2″−H2″ bonds is approximately 124° and dihedral angles between the P−O and C2″−C1″ and C2″−C3″ bonds are about 109° and 0°, respectively (*22*, *23*). In such an orientation, the phosphoryl group might form salt bridges with the kanamycin amines.

Prior to our work, regiospecificity of phosphoryl transfer had unambiguously been assigned by characterization of the products of the enzymic reaction only for two aminoglycoside phosphotransferases, APH(2″)-Ia and APH(3′)-IIIa (*7*, *8*, *24*). It was shown that the APH(2″)-Ia enzyme demonstrates extremely broad regiospecificity for phosphate transfer that reflects on the ability of the enzyme to modify at least four different hydroxyl groups of various aminoglycosides. Phosphorylation by this enzyme occurs at the 2″-OH of 4,6-disubstituted aminoglycosides (kanamycin A), while 4,5-disubstituted aminoglycosides are phosphorylated at position 5″ (lividomycin) or positions 3′ and 3‴ (neomycin). The APH(3′)-IIIa enzyme is also able to modify both the 4,6- and 4,5-disubstituted aminoglycosides. Phosphorylation of the 4,6-disubstituted aminoglycosides such as kanamycin A, gentamicin, and amikacin proceeds exclusively at the 3′-hydroxyl, while the 4,5-disubstituted aminoglycoside lividomycin, which lacks the 3′-hydroxyl, is modified at the 5″ hydroxyl (*25*, *26*). Regiospecificity of phosphate transfer by the APH(2″)-Ib enzyme had been predicted to be at the 2″-OH position, based only on the amino acid homology of this enzyme with the APH(2″)-Ia domain of the bifunctional enzyme AAC(6′)-Ie-APH(2″)-Ia. Our NMR studies of phosphorylated kanamycin unambiguously prove that the 2″-hydroxyl of this antibiotic is indeed the only group that is modified by the APH(2″)-Ib enzyme.

Table 1: Steady-State Kinetic Parameters for Catalysis by APH(2″)-Ib

substrate	K_m (μM)	k_{cat} (s^{-1})	k_{cat}/K_m (M^{-1} s^{-1})	K_i (μM)
kanamycin A	2.1 ± 0.1	45.0 ± 0.4	(2.2 ± 0.3) × 10^7	
tobramycin	1.5 ± 0.2	26.0 ± 0.5	(1.7 ± 0.4) × 10^7	
netilmicin	1.1 ± 0.1	19.1 ± 0.4	(1.7 ± 0.2) × 10^7	
dibekacin	1.2 ± 0.1	17.1 ± 0.1	(1.4 ± 0.3) × 10^7	
isepamicin	13.5 ± 1.1	5.7 ± 0.1	(4.4 ± 0.6) × 10^5	
amikacin	62.9 ± 8.3	8.3 ± 0.5	(1.3 ± 0.3) × 10^5	
arbekacin	3.1 ± 0.2	9.4 ± 0.1	(3.0 ± 0.5) × 10^6	
apramycin	29.6 ± 3.3	5.6 ± 0.1	(1.9 ± 0.2) × 10^5	
ATP	16.3 ± 1.6	43.3 ± 1.5	(2.7 ± 0.4) × 10^6	
neamine				0.26 ± 0.02
paromomycin				0.16 ± 0.09
lividomycin A				8.7 ± 1.5
streptomycin				169.5 ± 52

Steady-State Parameters. Different regiospecificity of phosphate transfer by APH(2″)-Ia, APH(3′)-IIIa, and APH(2″)-Ib enzymes reflects differences in their substrate profiles; while APH(2″)-Ia and APH(3′)-IIIa phosphorylate both the 4,6- and 4,5-disubstituted aminoglycosides, the latter are not substrates for the APH(2″)-Ib phosphotransferase (Table 1). Not unexpectedly, neamine, the 4,6-disubstituted aminoglycoside, composed of only two rings and devoid of the 2″-hydroxyl, is also not a substrate for the APH(2″)-Ib enzyme, but serves as a potent inhibitor (K_i value of 260 ± 20 nM; Table 1, Figure 2). Among all aminoglycosides tested, kanamycin A, tobramycin, netilmicin, and dibekacin are the best substrates. The APH(2″)-Ib catalyzed phosphorylation of these antibiotics with catalytic efficiencies (k_{cat}/K_m) of 1−2 × 10^7 M^{-1} s^{-1} (Table 1). These values indicate that the enzyme is extremely efficient at its function and might actually be operating at or near the diffusion limit. The catalytic efficiencies of the enzyme for three other 4,6-disubstituted aminoglycosides, arbekacin, isepamicin, and amikacin, are 7-, 50-, and 170-fold lower that that of kanamycin A. It is noteworthy that all three are the only 4,6-disubstituted aminoglycosides that have their N_1 of the 2-deoxystreptamine ring acylated by the *S*-4-amino-2-hydroxybutyryl group. The K_m values for 4,6-disubstituted 2-deoxystreptamines, with the exception of isepamicin and amikacin, are in the 1−3 μM range. Of the four 4,5-disubstituted aminoglycosides tested (paromomycin, lividomycin A, spectinomycin, and hygromycin B), none is a substrate for APH(2″)-Ib, but two of them (paromomycin and lividomycin A) are competitive inhibitors (K_i values 0.16 ± 0.09 and 8.7 ± 1.5 μM respectively; Table 1). We also studied the interaction of the APH(2″)-Ib enzyme with four atypical aminoglycosides (streptomycin, spectinomycin, apramycin, and hygromycin B) whose structures are different from both the 4,6- and 4,5-disubstituted aminoglycosides. Only one of those, apramycin, is a substrate for APH(2″)-Ib and one of them, streptomycin, is a poor inhibitor of the enzyme (Table 1). None of the inhibitors, apramycin, neamine, paromomycin, lividomycin A, and streptomycin, are slow-binding, but rather they are competitive linear inhibitors. Of the two other studied phosphotransferases from Gram-positive bacteria, APH(2″)-Ia and APH(3′)-IIIa, both exhibit a broader substrate profile but lower catalytic efficiency (k_{cat}/K_m values of 10^3−10^4 M^{-1} s^{-1} and 10^6 M^{-1} s^{-1}, respectively) than the APH(2″)-Ib enzyme.

Catalytic Mechanism. We started to investigate the kinetic mechanism of APH(2")-Ib by analyzing the initial velocity

Table 2: Dead-End and Product Inhibition of APH(2″)-Ib

variable substrate	inhibitor	inhibition pattern	K_{is} (μM)	K_{ii} (μM)
isepamicin	neamine	competitive	0.18 ± 0.04	
ATP	neamine	noncompetitive/mixed	0.23 ± 0.06	0.75 ± 0.07
isepamicin	AMP-PCP	noncompetitive/mixed	40 ± 5.9	187 ± 8
ATP	AMP-PCP	competitive	35 ± 4.6	
isepamicin	kanamycin phosphate	competitive	60.9 ± 1.5	
ATP	kanamycin phosphate	competitive	39.4 ± 9.3	

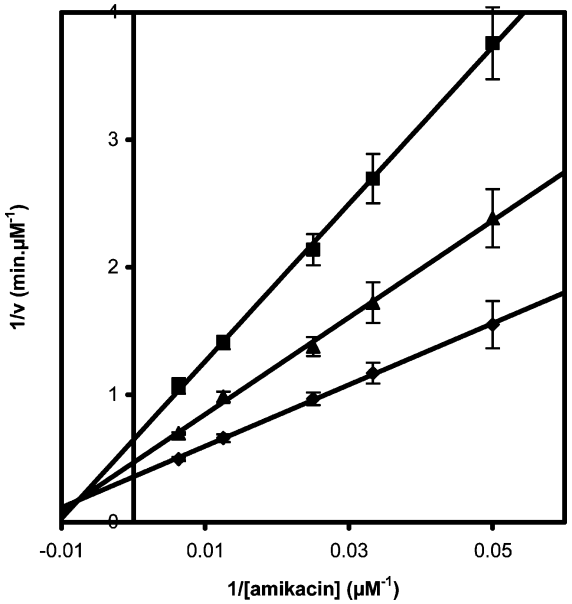

FIGURE 3: Initial velocity patterns for catalysis by APH(2″)-Ib. Initial velocity patterns for APH(2″)-Ib were obtained by measuring the rates of reaction at three different fixed concentrations of ATP, 8 μM (■), 16 μM (▲), and 32 μM (◆), and variable concentrations of amikacin (from 20 to 160 μM).

pattern. The velocity of reaction with aminoglycoside amikacin was determined at three fixed concentrations of ATP. Both substrates were used at concentrations that flanked their respective K_m values. All lines intersect to the left of the *y*-axis in the double-reciprocal plots of $1/v$ versus 1/[amikacin] (Figure 3). The observed pattern of intersecting lines in the double-reciprocal plots of $1/v$ versus 1/[amikacin] is indicative of a sequential mechanism (Figure 3). The data were also fit to both the sequential and the ping-pong mechanistic model with the Scientist software, using the k_{cat} and K_m parameters determined independently, which were allowed to vary up to 20% of their values. The mean sum of squared deviations was 50-fold larger for the ping-pong mechanism, which, unlike the sequential model, showed a systematic nonrandom trend in the residuals. The statistics of this fit indicate that the sequential model fits better the experimental data and excludes the possibility of the ping-pong mechanism (*27*). Sequential mechanism implies that both substrates (the aminoglycoside and ATP) have to be bound to the enzyme before the transfer of the phosphoryl group from ATP to aminoglycoside occurs. In fact, all aminoglycoside-modifying enzymes studied to date operate via a sequential mechanism (*4*, *28*−*34*). To distinguish between random and ordered binding of substrates, we carried out inhibition studies with the dead-end inhibitors neamine (aminoglycoside lacking 2″ hydroxyl) and AMP-PCP (nonhydrolyzable analogue of ATP). The dead-end inhibitor neamine behaved as a competitive inhibitor of

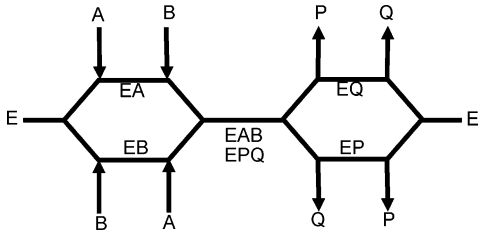

FIGURE 4: Schematic presentations of the proposed kinetic mechanisms of APH(2″)-Ib. A, aminoglycoside; B, ATP; P, aminoglycoside phosphate; Q, ADP.

isepamicin (K_{is} of 0.18 ± 0.04 μM) and noncompetitive/mixed inhibitor of ATP (K_{is} of 0.23 ± 0.06 μM and K_{ii} of 0.75 ± 0.07 μM; Table 3). In another set of experiments nonhydrolyzable nucleotide analogue AMP-PCP exhibited competitive inhibition versus ATP (K_{is} of 35 ± 4.6 μM) and noncompetitive/mixed inhibition versus isepamicin (K_{is} of 40 ± 5.9 μM and K_{ii} of 187 ± 8 μM). An inhibition pattern where the dead-end competitive inhibitor for either substrate is a noncompetitive/mixed inhibitor for the other substrate is indicative of the random Bi Bi mechanism (*35*). This mechanism implies that binding of substrates, aminoglycoside or ATP, to enzyme is random (Figure 4). In another set of experiments, kanamycin 2″-phosphate was used as a product inhibitor. Another product, ADP, could not be used in the coupled spectrophotometric assay because it is regenerated back to ATP during the reaction. We demonstrated that kanamycin 2″-phosphate is a competitive inhibitor for both the isepamicin (K_{is} of 60.9 ± 1.5 μM) and ATP (K_{is} of 39.4 ± 9.3 μM; Table 2) at unsaturated concentrations of fixed substrates, which is also in agreement with the random Bi Bi mechanism (*36*).

Chemical Mechanism. High k_{cat}/K_m values ($1-2 \times 10^7$ M^{-1} s^{-1}) obtained with the best aminoglycoside substrates could indicate that APH(2″)-Ib might actually be operating at or near the diffusion limit, where not a chemical step but rather the rate of diffusion of substrates or products limits the rate of phosphorylation. To investigate such a possibility, and to determine steps that are controlled by diffusion, we studied the effect of viscogens PEG 8000 (macroviscogen) and glycerol (microviscogen) on the APH(2″)-catalyzed phosphorylation of kanamycin A. Because viscogens can also influence the rate of the enzymatic reactions due to unpredictable perturbations of other parameters of the system, apart from just slowing down the diffusion rate, it is important to have proper controls when interpreting kinetic data measured in their presence (*37*). One way to account for such a possibility is to measure the reaction rates in the presence and absence of viscogens utilizing poor substrates, for which the chemical step is rate-limiting and change of diffusion rate is not expected to affect the overall rate of reaction (*38*, *39*). ATPγS could be such poor substrate because its sulfur-substituted phosphorus is less electrophilic than oxygen-

substituted phosphorus of ATP and this could result in a slower rate of catalysis. Thio effect is the ratio of the rate for the reaction with the phosphoryl group to the rate of the reaction with its thio analogue. We obtained the following parameters when ATP was used as a substrate in an uncoupled reaction: $K_m = 40.0 \pm 5.1$ μM, $k_{cat} = 7.6 \pm 0.6$ s^{-1}. When we used ATPγS as a substrate, corresponding parameters were $K_m = 45.8 \pm 5.8$ μM, $k_{cat} = 0.1 \pm 0.01$ s^{-1}. Thus, k_{cat} was attenuated 76-fold and k_{cat}/K_m 90-fold when ATPγS was used instead of ATP. These data indicate that ATPγS is a much worse substrate for APH(2″)-Ib than ATP and that the chemistry for ATPγS is at least partially rate-limiting. As anticipated, macroviscogen PEG had a negligible effect on the first (k_{cat}) and second order (k_{cat}/K_m) constants, when either kanamycin A or ATP was used as a variable substrate (Table 3). The values of k_{cat} and k_{cat}/K_m in the presence of microviscosogen glycerol were not changed when ATPγS was used as the variable substrate ($k_{cat}°/k_{cat}^{\eta} = -0.01 \pm 0.02$; $(k_{cat}/K_m)°/(k_{cat}/K_m)^{\eta} = -0.07 \pm 0.2$). On the other hand, in the presence of glycerol the slopes of the plots of $k_{cat}°/k_{cat}^{\eta}$ of kanamycin A and ATP versus relative viscosity are 1.15 ± 0.21 and 1.03 ± 0.16, respectively, while the slopes of the plots of $(k_{cat}/K_m)°/(k_{cat}/K_m)^{\eta}$ of kanamycin A and ATP versus relative viscosity are 0.73 ± 0.06 and 1.11 ± 0.14, respectively (Table 3). Significant changes in both k_{cat} and k_{cat}/K_m values in the presence of glycerol, when either kanamycin A or ATP concentrations were varied, indicate that product release and/or substrate binding are rate-limiting steps for APH(2″)-Ib-mediated catalysis.

To investigate the chemical mechanism of APH(2″)-Ib we evaluated solvent isotope on enzyme kinetics. Phosphorylation of aminoglycoside antibiotics by APH(2″)-Ib occurs by the attack of the 2″-hydroxyl of antibiotics on the γ-phosphate of ATP. In order to determine if proton transfer occurs in the transition state, we determined the k_{cat} values of kanamycin A in D_2O buffer. This results in exchange of the hydrogen on the substrate hydroxyl with deuterium. One would expect a significant solvent isotope effect on k_{cat} if deprotonation of the 2″-hydroxyl of an antibiotic is a rate-limiting step. Since the pK_a values of potentially important catalytic residues of enzymes are perturbed by D_2O, experiments had to be performed at two different pH values in H_2O buffer and two corresponding values in D_2O buffer (the pD values). To evaluate the solvent isotope effect on kinetics, we determined k_{cat} values for kanamycin A in deuterated buffer at pD 6.5 and pD 7.5 and compared them with the data obtained in nondeuterated buffer. We obtained k_{cat}^{H}/k_{cat}^{D} values of 1.0 ± 0.1 and 1.2 ± 0.1 at pH 6.5 and pH 7.5 correspondingly (Table 4). We also determined solvent deuterium isotope effect for ATPγS, for which the chemical step is rate-limiting. We first determined rates of APH(2″)-Ib-catalyzed phosphorylation of kanamycin at pH values between 6.5 and 7.5 and demonstrated that k_{cat} and K_m values for antibiotic are not changing significantly within this pH range ($k_{cat} = 48 \pm 5$; $K_m = 2.0 \pm 0.3$). Then measurements were performed at optimal pH/pD values (pH and pD = 7.0), and results demonstrated that substitution of deuterium for hydrogen had no effect on the k_{cat} value (k_{cat}^{H}/k_{cat}^{D} values of 1.0 ± 0.1). Thus, solvent isotope effect data do not suggest that proton transfer occurs in the rate-limiting transition state.

Concluding Remarks. Aminoglycoside antibiotics remain valuable and are sometimes indispensable for the treatment of various infections. Numerous representatives are classified into two major groups depending on whether they contain a 2-deoxystreptamine ring or not (the latter are often referred to as atypical aminoglycosides). Aminoglycosides belonging to the first group are further subdivided into 4,5− and 4,6-disubstituted compounds depending on the attachment of sugars to the 2-deoxystreptamine (Figure 2). Enzymatic modification of aminoglycoside antibiotics is the prevailing mechanism of bacterial resistance to this class of antimicrobial agents (*40*−*42*). Three distinct groups of enzymes, aminoglycoside phospho-, acetyl-, and nucleotidyltransferases, perform modification of the hydroxyl or amino groups of aminoglycosides important for efficient binding of the drug to its ribosomal target.

Seven distinct classes of aminoglycoside phosphotransferases that utilize ATP as the second substrate and are able to phosphorylate hydroxyl groups of various aminoglycoside antibiotics have been identified in clinical isolates and aminoglycoside-producing microorganisms (*5*). Two of the three aminoglycoside phosphotransferases whose kinetics have been studied, namely, APH(2″)-Ia and APH(3′)-Ia, follow the rapid-equilibrium random bi−bi mechanism (*4*, *33*), while another well-characterized phosphotransferase, (APH3′)-IIIa, was shown to operate via an ordered Theorell−Chance kinetic mechanism (*32*, *43*). Aminoglycoside phosphotransferase APH(2″)-Ib confers resistance to the clinically important aminoglycoside antibiotics gentamicin, tobramycin, netilmicin, isepamicin, and amikacin. Our studies with purified APH(2″)-Ib enzyme demonstrated that it phosphorylates the 4,6-disubstituted aminoglycosides, while 4,5-disubstituted antibiotics are not substrates for the enzyme. While the substrate profile of the APH(2″)-Ib is narrower than that of APH(2″)-Ia, its catalytic efficiency is 2 to 3 orders of magnitude higher. Results of our kinetics studies demonstrate that APH(2″)-Ib operates by the random Bi−Bi mechanism and diffusion-controlled substrate binding and/or product release is a rate-limiting step in the APH-(2″)-Ib-mediated catalytic reaction.

Table 3: Viscosity Effects on Catalysis by APH(2″)-Ib

viscogen	varied substrate	fixed substrate	$k_{cat}°/k_{cat}^{\eta}$ [a]	$(k_{cat}/K_m)°/(k_{cat}/K_m)^{\eta}$ [a]
glycerol	kanamycin A	ATP	1.15 ± 0.21	0.73 ± 0.06
glycerol	ATP	kanamycin A	1.03 ± 0.16	1.11 ± 0.14
PEG 8000	kanamycin A	ATP	0.01 ± 0.01	0.02 ± 0.01
PEG 8000	ATP	kanamycin A	0.03 ± 0.02	0.02 ± 0.02
glycerol	ATPγS	kanamycin A	-0.01 ± 0.02	-0.07 ± 0.2

[a] $k_{cat}°$ and $(k_{cat}/K_m)°$ are the rate constants with no viscogen added, and k_{cat}^{η} and $(k_{cat}/K_m)^{\eta}$ are the rate constants in the presence of viscogen.

Table 4: Solvent Isotope Effects in Catalysis by APH(2″)-Ib

	K_m (μM)	k_{cat} (s^{-1})	k_{cat}^{H}/k_{cat}^{D}	$(k_{cat}/K_m)^{H}/(k_{cat}/K_m)^{D}$
pH 6.5	1.9 ± 0.2	51.0 ± 6.1		
pD 6.5	12.9 ± 2.1	50.2 ± 6.2	1.0 ± 0.1	6.7 ± 0.9
pH 7.5	2.1 ± 0.3	38.3 ± 3.8		
pD 7.5	1.7 ± 0.2	31.3 ± 4.0	1.2 ± 0.1	1.0 ± 0.2

SUPPORTING INFORMATION AVAILABLE

TOCSY NMR spectra of phosphorylated kanamycin A and the graphs of inhibition patterns for APH(2”)-Ib. This

material is available free of charge via the Internet at http://pubs.acs.org.

REFERENCES

1. DiazGranados, C. A., Zimmer, S. M., Klein, M., and Jernigan, J. A. (2005) Comparison of mortality associated with vancomycin-resistant and vancomycin-susceptible enterococcal bloodstream infections: a meta-analysis, *Clin. Infect. Dis. 41*, 327−333.
2. Edmond, M. B., Wallace, S. E., McClish, D. K., Pfaller, M. A., Jones, R. N., and Wenzel, R. P. (1999) Nosocomial bloodstream infections in United States hospitals: a three-year analysis, *Clin. Infect. Dis. 29*, 239−244.
3. Ferretti, J. J., Gilmore, K. S., and Courvalin, P. (1986) Nucleotide sequence analysis of the gene specifying the bifunctional 6′-aminoglycoside acetyltransferase 2″-aminoglycoside phosphotransferase enzyme in *Streptococcus faecalis* and identification and cloning of gene regions specifying the two activities, *J. Bacteriol. 167*, 631−638.
4. Martel, A., Masson, M., Moreau, N., and Le Goffic, F. (1983) Kinetic studies of aminoglycoside acetyltransferase and phosphotransferase from *Staphylococcus aureus* RPAL. Relationship between the two activities, *Eur. J. Biochem. 133*, 515−521.
5. Shaw, K. J., Rather, P. N., Hare, R. S., and Miller, G. H. (1993) Molecular genetics of aminoglycoside resistance genes and familial relationships of the aminoglycoside-modifying enzymes, *Microbiol. Rev. 57*, 138−163.
6. Leclercq, R., Dutka-Malen, S., Brisson-Noel, A., Molinas, C., Derlot, E., Arthur, M., Duval, J., and Courvalin, P. (1992) Resistance of enterococci to aminoglycosides and glycopeptides, *Clin. Infect. Dis. 15*, 495−501.
7. Azucena, E., Grapsas, I., and Mobashery, S. (1997) Properties of a bifunctional bacterial antibiotic resistance enzyme that catalyzes ATP-dependent 2″-phosphorylation and acetyl-CoA-dependent 6′-acetylation of aminoglycosides, *J. Am. Chem. Soc. 119*, 2317−2318.
8. Daigle, D. M., Hughes, D. W., and Wright, G. D. (1999) Prodigious substrate specificity of AAC(6′)-APH(2″), an aminoglycoside antibiotic resistance determinant in enterococci and staphylococci, *Chem. Biol. 6*, 99−110.
9. Tsai, S. F., Zervos, M. J., Clewell, D. B., Donabedian, S. M., Sahm, D. F., and Chow, J. W. (1998) A new high-level gentamicin resistance gene, *aph(2″)-Id*, in *Enterococcus* spp, *Antimicrob. Agents Chemother. 42*, 1229−1232.
10. Kao, S. J., You, I., Clewell, D. B., Donabedian, S. M., Zervos, M. J., Petrin, J., Shaw, K. J., and Chow, J. W. (2000) Detection of the high-level aminoglycoside resistance gene *aph(2″)-Ib* in *Enterococcus faecium*, *Antimicrob. Agents Chemother. 44*, 2876−2879.
11. Chow, J. W., Zervos, M. J., Lerner, S. A., Thal, L. A., Donabedian, S. M., Jaworski, D. D., Tsai, S., Shaw, K. J., and Clewell, D. B. (1997) A novel gentamicin resistance gene in Enterococcus, *Antimicrob. Agents Chemother. 41*, 511−514.
12. Kim, C., Haddad, J., Vakulenko, S. B., Meroueh, S. O., Wu, Y., Yan, H., and Mobashery, S. (2004) Fluorinated aminoglycosides and their mechanistic implication for aminoglycoside 3′-phosphotransferases from Gram-negative bacteria, *Biochemistry 43*, 2373−2383.
13. Bodenhausen, G., Freeman, R., Niedermeyer, R., and Turner, D. L. (1977) Double fourier transformation in high-resolution NMR, *J. Magn. Reson. 26*, 133−164.
14. Bax, A., Griffey, R. H., and Hawkins, B. L. (1983) Correlation of proton and N-15 chemical-shifts by multiple quantum NMR, *J. Magn. Reson. 55*, 301−315.
15. Bax, A., and Morris, G. A. (1981) An improved method for heteronuclear chemical-shift correlation by two-dimensional NMR, *J. Magn. Reson. 42*, 501−505.
16. Bax, A., and Summers, M. F. (1986) H-1 and C-13 assignments from sensitivity-enhanced detection of heteronuclear multiple-bond connectivity by 2D multiple quantum NMR, *J. Am. Chem. Soc. 108*, 2093−2094.
17. Griesinger, C., Otting, G., Wuthrich, K., and Ernst, R. R. (1988) Clean TOCSY for H-1 spin system-identification in macromolecules, *J. Am. Chem. Soc. 110*, 7870−7872.
18. Wijmenga, S. S., Hallenga, K., and Hilbers, C. W. (1989) A 3-dimensional heteronuclear multiple-quantum coherence homonuclear Hartmann-Hahn experiment, *J. Magn. Reson. 84*, 634−642.
19. Wishart, D. S., Bigam, C. G., Yao, J., Abildgaard, F., Dyson, H. J., Oldfield, E., Markley, J. L., and Sykes, B. D. (1995) H-1, C-13 and N-15 chemical-shift referencing in biomolecular NMR, *J. Biomol. NMR 6*, 135−140.
20. Lide, D. R. (2004) *Handbook of chemistry and physics*, 85th ed., Section 8, pp 58−84, CRC Press, Boca Raton, FL.
21. Morrison, J. F. (2001) Enzyme activity: Reversible inhibition, *Encycl. Life Sci.* 1−8.
22. Breg, J., Romijn, D., Vanhalbeek, H., Vliegenthart, J. F. G., Visser, R. A., and Haasnoot, C. A. G. (1988) Characterization of 4 Lactose Monophosphates by Application of P-31-NMR, C-13-NMR, and H-1-NMR Spectroscopy, *Carbohydr. Res. 174*, 23−36.
23. Lankhorst, P. P., Haasnoot, C. A. G., Erkelens, C., and Altona, C. (1984) Nucleic-Acid Constituents. 36. C-13 NMR in Conformational-Analysis of Nucleic-Acid Fragments. 2. A Reparametrization of the Karplus Equation for Vicinal NMR Coupling-Constants in CCOP and HCOP Fragments, *J. Biomol. Struct. Dyn. 1*, 1387−1405.
24. Kondo, S., Tamura, A., Gomi, S., Ikeda, Y., Takeuchi, T., and Mitsuhashi, S. (1993) Structures of enzymatically-modified products of arbekacin by methicillin-resistant *Staphylococcus aureus*, *J. Antibiot. 46*, 310−315.
25. Mckay, G. A., Robinson, R. A., Lane, W. S., and Wright, G. D. (1994) Active-site labeling of an aminoglycoside antibiotic phosphotransferase (APH(3′)-IIIa), *Biochemistry 33*, 14115−14120.
26. Thompson, P. R., Hughes, D. W., and Wright, G. D. (1996) Mechanism of aminoglycoside 3′-phosphotransferase type IIIa: His188 is not a phosphate-accepting residue, *Chem. Biol. 3*, 747−755.
27. Mannervik, B. (1982) Regression-Analysis, Experimental Error, and Statistical Criteria in the Design and Analysis of Experiments for Discrimination between Rival Kinetic-Models, *Methods Enzymol. 87*, 370−390.
28. Jana, S., and Deb, J. K. (2005) Kinetic mechanism of streptomycin adenylyltransferase from a recombinant *Escherichia coli*, *Biotechnol. Lett. 27*, 519−524.
29. Kim, C., Hesek, D., Zajicek, J., Vakulenko, S. B., and Mobashery, S. (2006) Characterization of the bifunctional aminoglycoside-modifying enzyme ANT(3″)-Ii/AAC(6′)-IId from *Serratia marcescens*, *Biochemistry 45*, 8368−8377.
30. Chen-Goodspeed, M., Vanhooke, J. L., Holden, H. M., and Raushel, F. M. (1999) Kinetic mechanism of kanamycin nucleotidyltransferase from *Staphylococcus aureus*, *Bioorg. Chem. 27*, 395−408.
31. Draker, K. A., Northrop, D. B., and Wright, G. D. (2003) Kinetic mechanism of the GCN5-related chromosomal aminoglycoside acetyltransferase AAC(6′)-Ii from *Enterococcus faecium*: evidence of dimer subunit cooperativity, *Biochemistry 42*, 6565−6574.
32. McKay, G. A., and Wright, G. D. (1995) Kinetic mechanism of aminoglycoside phosphotransferase type IIIa. Evidence for a Theorell-Chance mechanism, *J. Biol. Chem. 270*, 24686−24692.
33. Siregar, J. J., Miroshnikov, K., and Mobashery, S. (1995) Purification, characterization, and investigation of the mechanism of aminoglycoside 3′-phosphotransferase type Ia, *Biochemistry 34*, 12681−12688.
34. Magnet, S., Lambert, T., Courvalin, P., and Blanchard, J. S. (2001) Kinetic and mutagenic characterization of the chromosomally encoded *Salmonella enterica* AAC(6′)-Iy aminoglycoside N-acetyltransferase, *Biochemistry 40*, 3700−3709.
35. Fromm, H. J. (1979) Use of competitive inhibitors to study substrate binding order, *Methods Enzymol. 63*, 467−486.
36. Rudolph, F. B. (1979) Product inhibition and abortive complex formation, *Methods Enzymol. 63*, 411−436.
37. Blacklow, S. C., Raines, R. T., Lim, W. A., Zamore, P. D., and Knowles, J. R. (1988) Triosephosphate Isomerase Catalysis Is Diffusion Controlled - Appendix - Analysis of Triose Phosphate Equilibria in Aqueous-Solution by P-31 NMR, *Biochemistry 27*, 1158−1167.
38. Hardy, L. W., and Kirsch, J. F. (1984) Diffusion-Limited Component of Reactions Catalyzed by Bacillus-Cereus Beta-Lactamase-I, *Biochemistry 23*, 1275−1282.
39. Brouwer, A. C., and Kirsch, J. F. (1982) Investigation of Diffusion-Limited Rates of Chymotrypsin Reactions by Viscosity Variation, *Biochemistry 21*, 1302−1307.
40. Eliopoulos, G. M., Farber, B. F., Murray, B. E., Wennersten, C., and Moellering, R. C., Jr. (1984) Ribosomal resistance of clinical enterococcal isolates to streptomycin, *Antimicrob. Agents Chemother. 25*, 398−399.

41. Coque, T. M., Arduino, R. C., and Murray, B. E. (1995) High-level resistance to aminoglycosides - Comparison of community and nosocomial fecal isolates of enterococci, *Clin. Infect. Dis. 20*, 1048−1051.
42. Vakulenko, S. B., and Mobashery, S. (2003) Versatility of aminoglycosides and prospects for their future, *Clin. Microbiol. Rev. 16*, 430−450.
43. McKay, G. A., and Wright, G. D. (1996) Catalytic mechanism of enterococcal kanamycin kinase (APH(3′)-IIIa): viscosity, thio, and solvent isotope effects support a Theorell-Chance mechanism, *Biochemistry 35*, 8680−8685.

BI6024512